Heliyon 7 (2021) e08078

Contents lists available at ScienceDirect

Heliyon

journal homepage: www.cell.com/heliyon

Research article

# Computational study and *in vitro* alpha-glucosidase inhibitory effects of medicinal plants from a Thai folk remedy

Komgrit Eawsakul [a], Pharkphoom Panichayupakaranant [b], Tassanee Ongtanasup [a], Sakan Warinhomhoun [a], Kunwadee Noonong [d], Kingkan Bunluepuech [a,c,*]

[a] *School of Medicine, Research Excellence Center for Innovation and Health Product Walailak University, Nakhon Si Thammarat, 80160, Thailand*
[b] *Phytomedicine and Pharmaceutical Biotechnology Excellence Center, Faculty of Pharmaceutical Sciences, Prince of Songkla University, Hat-Yai, Songkhla 90112, Thailand*
[c] *Faculty of Traditional Thai Medicine Prince of Songkla University, Hat Yai, Songkhla, 90112, Thailand*
[d] *School of Allied Health Sciences, Walailak University, Thailand*

ARTICLE INFO

*Keywords:*
Thai folk remedy
Alpha-glucosidase inhibitory
Computational study

ABSTRACT

The number of patients with type 2 diabetes mellitus (T2DM) has increased worldwide. Although an instant cure was achieved with the standard treatment acabose, unsatisfactory symptoms associated with cardiovascular disease after acabose administration have been reported. Therefore, it is important to explore new treatments. A Thai folk recipe has long been used for T2DM treatment, and it effectively decreases blood glucose. However, the mechanism of this recipe has never been proven. Therefore, the potential anti-T2DM effect of this recipe, which is used in Thai hospitals, was determined to involve alpha-glucosidase (AG) inhibition with a half maximal inhibitory concentration ($IC_{50}$). *In vitro* experiments showed that crude *Cinnamomum verum* extract ($IC_{50} = 0.35 \pm 0.12$ mg/mL) offered excellent inhibitory activity, followed by extracts from *Tinospora crispa* ($IC_{50} = 0.69 \pm 0.39$ mg/mL), *Stephania suberosa* ($IC_{50} = 1.50 \pm 0.17$ mg/mL), *Andrographis paniculate* ($IC_{50} = 1.78 \pm 0.35$ mg/mL), and *Thunbergia laurifolia* ($IC_{50} = 4.66 \pm 0.27$ mg/mL). However, the potencies of these extracts were lower than that of acabose ($IC_{50} = 0.55 \pm 0.11$ mg/mL). Therefore, this study investigated and developed a formulation of this recipe using computational docking. Among 61 compounds, 7 effectively inhibited AG, including chlorogenic acid ($IC_{50} = 819.07$ pM) through 5 hydrogen bonds (HBs) and 2 hydrophobic interactions (HIs); β-sitosterol ($IC_{50} = 4.46$ nM, 6 HIs); ergosterol peroxide ($IC_{50} = 4.18$ nM, 6 HIs); borapetoside D ($IC_{50} = 508.63$ pM, 7 HBs and 2 HIs); borapetoside A ($IC_{50} = 1.09$ nM, 2 HBs and 2 His), stephasubimine ($IC_{50} = 285.37$ pM, 6 HIs); and stephasubine ($IC_{50} = 1.09$ nM, 3 HBs and 4 HIs). These compounds bind with high affinity to different binding pockets, leading to additive effects. Moreover, the pharmacokinetics of six of these seven compounds (except ergosterol peroxide) showed poor absorption in the gastrointestinal tract, which would allow for competitive binding to AG in the small intestine. These results indicate that the development of these 6 compounds into oral antidiabetic agents is promising.

## 1. Introduction

Diabetes mellitus (DM) is a chronic disease caused by high glucose levels in the bloodstream. The number of patients who are affected by type 2 diabetes (T2D) is estimated to be approximately 415 million worldwide [1, 2]. The number of patients with diabetes is predicted to reach 642 million in 2040 [3]. All patients diagnosed with T2D have complications, such as nephropathy, retinopathy, and cardiovascular disorders [4]. To date, strategies to control glucose levels in the bloodstream include inhibition of the digestion of carbohydrates, polysaccharides, and disaccharides [5, 6, 7]. The enzyme alpha-glucosidase (AG) plays an important role in starch digestion into glucose. Therefore, glucose levels should be maintained at less than 200 mg/dl when detected any time of the day without fasting [8].

AG is an enzyme that hydrolyzes α(1→4) monosaccharide bonds, leading to glucose absorption and hyperglycemia [9]. This enzyme is secreted in the small intestine [10]. Thus, AG directly increases glucose levels in the bloodstream. To control normal blood glucose levels for diabetes treatment, many studies have shown that the inhibition of AG is a potential therapeutic strategy [6, 11]. However, the limitations of

* Corresponding author.
*E-mail address:* kingkan.bu@wu.ac.th (K. Bunluepuech).

https://doi.org/10.1016/j.heliyon.2021.e08078
Received 2 June 2021; Received in revised form 6 September 2021; Accepted 24 September 2021

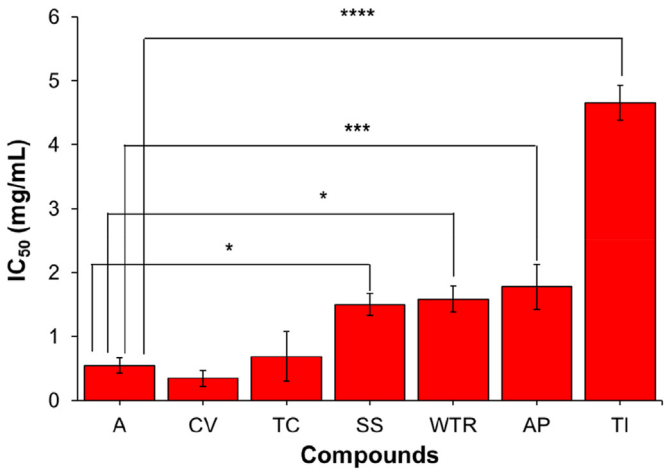


**Figure 1.** Comparison of AG inhibitory activity of each Thai herb extract in ethanol and acabose (positive control) in vitro.

**Table 1.** Comparison of AG inhibitory activity of the Thai herbal recipe, *T. crispa* and *C. verum* extracted in ethanol, water and chloroform.

| Sample | $IC_{50}$ (mg/mL) |
|---|---|
| Thai recipe extracted in ethanol | 15.90 ± 1.51 |
| Thai recipe extracted in water | 18.17 ± 1.03 |
| Thai recipe extracted in chloroform | 14.99 ± 0.99 |
| *T. crispa* extracted in ethanol | 0.69 ± 0.39 |
| *T. crispa* extracted in water | 1.14 ± 0.11 |
| *T. crispa* extracted in chloroform | 0.66 ± 0.10 |
| *C. verum* extracted in ethanol | 0.35 ± 0.12 |
| *C. verum* extracted in water | 0.05 ± 0.02 |
| *C. verum* extracted in chloroform | 0.68 ± 0.08 |

**Table 2.** Molecular docking results and predicted $IC_{50}$ values of AG inhibitory activity of acabose (positive control).

| Medicinal plant part | Ligand | Binding energy (kcal/mol) | | | Anti-diabetes activity $IC_{50}$ |
|---|---|---|---|---|---|
| | | Arguslab | Autodock Vina | Autodock | |
| | Acabose | -7.58662 | -8.1 | -9.1 | 212.84 nM |

available antidiabetic compounds, such as miglitol, metformin, and acarbose, are serious side effects, including gastrointestinal problems in response to disturbances in microbiota, such as Lactobacillaceae, Ruminococcaceae, and Veillonellaceae [12].

To prevent these side effects, a Thai herbal recipe composed of 36% *Andrographis paniculata*, 36% *Thunbergia laurifolia*, 9.3% *Tinospora crispa* L, 9.3% *Stephania suberosa* and 9.3% *Cinnamomum verum* was used in this study to reduce blood sugar. This Thai herbal recipe is used in traditional Thai medicine hospitals, and it originated from Dr. Wirot Bunluepuech, who practices traditional Thai medicine in Nakhon Si Thammarat Province. According to diabetes treatment results from Thai Traditional Medical Hospital, the blood glucose levels of patients were first monitored by fingertip blood sampling. Blood glucose levels gradually decreased after 5 bolus doses of this herbal recipe after breakfast and dinner. After 1 month, the blood glucose levels of the patients decreased from 245 mg/dl to 205 mg/dl. By month 2, the blood glucose levels further decreased to 167 mg/dl. In the third month, the blood glucose levels decreased to 148 mg/dl, and blood glucose remained at this level during the 4th and fifth months. Throughout five months of monitoring, the symptoms of fatigue, frequency of urination at night and thirst gradually decreased until no signs of fatigue were reported and waking at night to urinate no longer occurred.

*A. paniculata* of the Acanthaceae family is known in Thai as Fah Talai Joan, and the aerial part is used to treat tonsillitis, dysentery, diarrhea and fever [13]. *A. paniculata* and andrographolide show appreciable AG inhibitory effects [14], including in rats [15], in addition to showing hypoglycemic [16], antibacterial, antiviral [17], anti-inflammatory [18], antimalarial [19], immunostimulatory [20], hepatoprotective [21], antithrombotic [22], and anticancer [23] activities.

The leaves and stems of *T. laurifolia* of the Acanthaceae family are used as antidotes against several poisonous agents in traditional Thai medicine. The Thai name for this plant is Rang Jert, and the dried root is also used as an anti-inflammatory agent [13]. *T. laurifolia* leaves have antioxidant, antimicrobial, detoxifying, and antidiabetic activities without toxic effects [24]. Additional biological activities, such as antioxidant, anti-inflammatory, and hepatoprotective effects, have been found from *T. laurifolia* [25].

*T. crispa* is a medicinal plant belonging to the botanical family Menispermaceae, and the local name is boraphet. The stems of *T. crispa* are used to treat fever, as a health tonic, and to increase bile function [13]. It is also used in Malaysia as a remedy for patients with DM [26]. *T. crispa* has antihyperglycemic effects in animals [27]. The hypoglycemic effects of *T. crispa* are mediated by an increase in insulin secretion from isolated rat and human islets of Langerhans [27].

*S. suberosa* is a medicinal plant belonging to the botanical family Menispermaceae, and it is commonly used for the treatment of a variety of aliments under the local name boraphet phungchang. Its stems are used to treat diabetes and anemia, and it is used as a health tonic and longevity agent. Many of the plants from the *Stephania* genus show biological activities, including antitumor and emetine-type activities [28].

*C. verum* is a medicinal plant belonging to the Lauraceae botanical family, and its bark is used to treat exhaustion, as a health tonic, and to nourish the mind [13]. *C. verum* consumption is associated with an attenuation of DM [29]. *C. verum* effectively lowered fasting blood glucose levels in diet-induced obese hyperglycemic mice [30] and lowered hemoglobin A1C in patients with T2D [31].

The present study used various photochemical methods to analyze and derive the 3D structures of 22 compounds from *A. paniculate*, 4 from *T. laurifolia*, 9 from *T. crispa* L, 11 from *S. suberosa* and 15 from *C. verum* and examined the effects of these compounds on blood glucose levels and the inhibition of AG using AutoDock, AutoDock Vina and ArgusLab [32, 33, 34, 35, 36]. Chemical binding was visualized by Discovery Studio [37]. The absorption ability from the gastrointestinal (GI) tract was predicted by calculating the hydrophobicity and hydrophilicity of the compounds using the BOILED-Egg model [38]. Notably, a suitable compound should be absorbed to a lesser extent in the GI tract because AG is released in the small intestine.

Selection of the correct solvent is important to enhance the yield of the selected compounds. The solubility of the solute in the solvent is a key parameter that defines the extraction yield. The capability of the solvent to dissolve the selected compounds may be predicted by the physical properties and chemical parameters of the compound, such as its solubility, dielectric constant, and number of donor and receptor hydrogens [39]. Natural compounds generally exhibit good solubility in highly polar solvents, with Hildebrand solubility parameters between 20 and 30 $MPa^{1/2}$ [40]. Therefore, the solvent solubility parameter corresponding to the compound solubility at its maximum curve was considered. Several recent methods can predict the solubility of compounds in solvents and are described below.

1) Regular solution theory was used to predict the solubility of compounds in a solvent via a quadratic logarithm [40]. The solubility of a compound in a solvent is plotted as a bell shape. The maximum amount of compound that can be dissolved in the solvent is found at the top of the bell. However, the solubility of some compounds cannot be predicted using this method. The melting temperature ($T_m$),

**Table 3.** Molecular docking results and predicted $IC_{50}$ values of AG inhibitory activity of 21 *Andrographis paniculate* extracts.

| Medicinal plant part | Ligand | Binding energy (kcal/mol) | | | Anti-diabetes activity $IC_{50}$ |
|---|---|---|---|---|---|
| | | Arguslab | Autodock Vina | Autodock | |
| Aerial plant | β-sitosterol | -14.0171 | -8.2 | -11.39 | 4.46 nM |
| Aerial plant | 2-cis-6-trans-Farnesol | -13.4968 | -6.4 | 7.72 | 2.18 μM |
| Aerial plant | Stigmasterol | -12.2568 | -8.9 | -11.08 | 7.57 nM |
| Leaves | Andrograpanin | -11.9754 | -7.6 | 9.36 | 138.58 nM |
| Aerial plant | Ergosterol peroxide | -10.7027 | -9.6 | -11.43 | 4.18 nM |
| Leaves | Caffeic acid | -10.451 | -6.4 | -8.74 | 393.91 nM |
| Aerial parts | Andrographolactone | -10.3188 | -8.1 | -9.65 | 84.76 nM |
| Aerial plant | 14-Deoxy-11,12-didehydrographolide | -9.7979 | -8.0 | -9.43 | 122.97 nM |
| Aerial plant | 14-Deoxyandrographolide | -9.71145 | -7.6 | -9.59 | 93.48 nM |
| Leaves/aerial | Andrographolide | -9.66208 | -8.1 | -10.98 | 9.0 nM |
| Aerial plant | Neoandrographolide | -9.65087 | -8.4 | -12.02 | 1.55 nM |
| Leaves | Paniculide A | -9.36806 | -7.1 | -9.26 | 163.48 nM |
| Aerial plant | 5-Hydroxy-7,8-dimethoxyflavanone | -9.30062 | -7.2 | -9.68 | 80.6 nM |
| Leaves/aerial | Andrographoside | -9.19261 | -8.5 | -12.05 | 1.47 nM |
| Whole plant | Dihydroskullcapflavone | -9.08818 | -7.2 | -10.05 | 43.26 nM |
| Whole plant | 7-O-Methylwogonin | -8.89015 | -7.0 | -9.36 | 138.55 nM |
| Root | Apigenin-7,4-dimethyl ether | -8.65278 | -8.1 | -10.25 | 30.45 nM |
| Whole plant | 5,7,2′,3′-Tetramethoxyflavone | -8.43209 | -7.6 | -9.78 | 67.23 nM |
| Whole plant | 5-Hydroxy-7,8,2,5′-tetramethoxyflavone | -8.09755 | -7.8 | -10.16 | 35.58 nM |
| Root | 1,2-Dihydroxy-6,8-dimethoxy-xanthone | -8.00743 | -7.1 | -9.59 | 92.67 nM |
| Root | 5-hydroxy-7, 2′, 6'trimethoxyflavone | -7.71015 | -7.6 | -9.85 | 60.32 nM |

**Table 4.** Molecular docking results and predicted $IC_{50}$ values of AG inhibitory activity of 9 *Tinospora crispa* extracts.

| Medicinal plant part | Ligand | Binding energy (kcal/mol) | | | Anti-diabetes activity $IC_{50}$ |
|---|---|---|---|---|---|
| | | Arguslab | Autodock Vina | Autodock | |
| Stem | Tyramine | -9.82256 | -5.6 | -6.86 | 9.38 μm |
| Stem | Borapetoside D | -9.69868 | -8.2 | -12.68 | 508.63 pM |
| Stem | Higenamine | -9.55481 | -7.9 | -9.27 | 159.03 nM |
| Stem | Borapetoside A | -9.12845 | -9.2 | -12.22 | 1.09 nM |
| Stem | Borapetoside E | -8.9324 | -8.2 | -11.7 | 2.65 nM |
| Stem | Borapetol B | -8.76361 | -8.3 | -10.86 | 11 nM |
| Stem | Syringin | -8.63661 | -6.8 | -9.81 | 64.43 nM |
| Stem | Salsolinol | -8.253 | -6.3 | 9.31 | 150.01 nM |
| Vines | Adenosine | -7.68071 | -7.0 | -10.24 | 31.24 nM |

current temperature (T), heat of fusion ($H_f$), solid solubility ($X_i$), and interactions between the solvent and solute ($\gamma_i$) parameters were used to calculate the solubility using Eq. (1).

$$\ln X_i = \frac{Hf}{RTm}\left(1 - \frac{Tm}{T}\right) - \ln\gamma_i \quad (1)$$

2) The Car-Parrinello method is a molecular dynamic simulation that is generally used to simulate and calculate the compatibility of compounds and solvents [41]. However, calculations from this method may be incorrect due to the large number of solvents, which leads to interference with quantum chemical calculations.
3) The quantitative structure-property relationship (QSPR) method has been employed to predict the aqueous solubility (log S), octanol-water partition coefficient, and energy of molecular orbitals. The solubility of a compound can also be predicted computationally using the mathematical software COSMOquick. The COSMOquick approach uses a QSPR technique to estimate the solubility [42]. In this study,

**Table 5.** Molecular docking results and predicted $IC_{50}$ values of AG inhibitory activity of 11 *Stephania suberosa* extracts.

| Medicinal plant part | Ligand | Binding energy (kcal/mol) | | | Anti-diabetes activity $IC_{50}$ |
|---|---|---|---|---|---|
| | | Arguslab | Autodock Vina | Autodock | |
| Stem | Stephasubine | -9.10172 | -9.0 | -12.62 | 560.6 pM |
| Stem | Tetrahydrostephabine | -8.82366 | -7.5 | -9.65 | 84.11 nM |
| Stem | Tetrahydropalmatine | -8.77644 | -7.6 | -10.03 | 44.33 nM |
| Stem | Discretine | -8.72261 | -8.4 | -9.58 | 95.41 nM |
| Stem | Corytenchine | -8.6583 | -7.9 | -9.92 | 53.52 nM |
| Stem | Capaurimine | -8.60319 | -7.8 | -9.6 | 91.76 nM |
| Stem | Coreximine | -8.48967 | -8.4 | -9.74 | 72.19 nM |
| Stem | 8-Oxypseudopalmatine | -8.32913 | -7.5 | -10.12 | 38.01 nM |
| Stem | Stephasubimine | -8.31026 | -9.7 | -13.02 | 285.37 pM |
| Stem | Tetrahydrostephabine | -7.83637 | -7.5 | -9.65 | 84.11 nM |
| Stem | Cepharanthine | -6.44155 | -9.3 | -11.17 | 6.48 nM |

**Table 6.** Molecular docking results and predicted $IC_{50}$ values of AG inhibitory activity of 4 *Thumbergia laurifolia* extracts.

| Medicinal plant part | Ligand | Binding energy (kcal/mol) | | | Anti-diabetes activity $IC_{50}$ |
|---|---|---|---|---|---|
| | | Arguslab | Autodock Vina | Autodock | |
| Leaves and Flowers | Apigenin | -8.96918 | -7.9 | -10.41 | 23.37 nM |
| Leaves and Flowers | Gallic acid | -8.96747 | -5.8 | -9.12 | 207.47 nM |
| Leaves | (E)-2-Hexenyl-β-glucopyranoside | -8.85008 | -6.2 | -9.25 | 166.58 nM |
| Leaves and Flowers | Protocatechuic acid | -6.79875 | -5.8 | -8.0 | 1.37 μM |

**Table 7.** Molecular docking results and predicted $IC_{50}$ values of AG inhibitory activity of 16 *Cinnamom verum* extracts.

| Medicinal plant part | Ligand | Binding energy (kcal/mol) | | | Anti-diabetes activity $IC_{50}$ |
|---|---|---|---|---|---|
| | | Arguslab | Autodock Vina | Autodock | |
| Bark | Cinnamyl acetate | -11.6707 | -6.0 | -6.92 | 8.41 μM |
| Bark | Cinnamyl alcohol | -11.3348 | -5.8 | -6.7 | 12.36 μM |
| Leaf | (E)-Cinnemaldehyde | -11.2721 | -5.8 | -6.72 | 11.87 μM |
| Bark | P-Cymene | -11.0936 | -6.2 | -6.68 | 12.71 μM |
| Bark | γ–Terpinene | -11.0464 | -6.2 | -7.2 | 5.25 μM |
| Bark | β-Caryophyllene | -9.96724 | -6.2 | -7.28 | 4.64 μM |
| Bark | α-Phellandrene | -9.46863 | -6.1 | -6.98 | 7.65 μM |
| Bark | Linalool | -9.28838 | -5.8 | -6.84 | 9.73 μM |
| Bark | Camphene | -9.26225 | -5.2 | -6.03 | 38.18 μM |
| Bark | α–Pinene | -9.21657 | -6.0 | -6.23 | 27.2 μM |
| Leaf | Eugenol | -9.19535 | -5.7 | -7.11 | 6.1 μM |
| Bark | Benzaldehyde | -9.01411 | -4.8 | -5.56 | 84.55 μM |
| Bark | β-Pinene | -8.9636 | -5.1 | -6.34 | 22.49 μM |
| Bark | Linalyl oxide | -7.9782 | -6.1 | -6.53 | 16.4 μM |
| Bark | Thiazole | -6.27006 | -2.9 | -4.36 | 632.21 μM |
| Bark | Chlorogenic acid | -10.6808 | -8.1 | -12.4 | 819.07 pM |

the free energy of fusion ($\Delta G_{fus}$) was calculated according to the following Eq. (2):

$$\Delta G_{fus} = \Delta H_{fus} - \Delta H_{fus}\,(1 - T)/T_m \quad (2)$$

where $\Delta H_{fus}$ is the enthalpy of fusion, T is room temperature, and $T_m$ is the melting temperature of the compound. These values were efficiently estimated using COSMOquick. Therefore, this method was used to select the extraction solvent for the compounds that would produce high yields.

The purpose of this research was to develop a more effective Thai traditional recipe for reducing blood sugar over a long time through computer simulation and to select the best extraction method to extract for inhibiting AG enzymes, which cause diabetes.

## 2. Materials and methods

### 2.1. Materials

The following software were used in the present study: i) AutoDock 1.5.6, ii) Python 3.8.2, iii) MGLTools 1.5.4 iv) Discovery Studio-2017, v) ArgusLab 4.0.1, vi) ChemSketch, vii)Avogadro, viii) OpenBabel, ix) SwissADME: a free web tool to evaluate pharmacokinetics. The following were the system properties with which the study was conducted. Processor: Intel Xeon-E5-2678v3 12C/24T CPU @ 2.50 GHz -3.10 GHz processor, system memory: 32 GB RAM DDR4-2133 RECC, graphics processing: VGA GTX 1070 TI 8G, system type: 64-bit operating system, Windows 10 as Operating System. These requirements were prescribed in the software manual for the compatibility of the above-mentioned software. All solvents for extraction and isolation processes were purchased from Thail Oil Co. Ltd., Thailand. Alpha-glucosidase from Saccharomyces cerevisieae, para–nitrophenyl–alpha–D– glucopyranosidse and acarbose were obtained from Sigma-Aldrich, Germany.

### 2.2. Crude extract preparation

The medicinal plants in the drug formulas were composed of the following 5 herbs: *A. paniculate*, *T. crispa*, *S. suberosa*, *T. laurifolia*, and *C. verum*. Voucher specimens of *A. paniculate* SM0114161404, *T. crispa* SM20090318, *S. suberosa* SM19201921. *T. laurifolia* SM 20081201, and *C. verum* SM 03092205 are deposited at the Botanic Garden, Walailak University, Nakhon Si Thammarat, Thailand.

**Table 8.** Chemical interaction analyses of the inhibitory activity of *β*-sitosterol against AG using Discovery Studio.

| Receptor (amino acid) | Distance (Å) | Ligand (group) | Receptor (group) | Chemical interaction |
|---|---|---|---|---|
| MET 385 | 4.81486 | Alkyl | Alkyl | Hydrophobic |
| ILE 143 | 5.14935 | Alkyl | Alkyl | Hydrophobic |
| HIS 203 | 5.39158 | Pi-Orbitals | Alkyl | Hydrophobic |
| PHE 282 | 5.19065 | Pi-Orbitals | Alkyl | Hydrophobic |
| TYR 388 | 5.37431 | Pi-Orbitals | Alkyl | Hydrophobic |
| TYR 388 | 4.80415 | Pi-Orbitals | Alkyl | Hydrophobic |

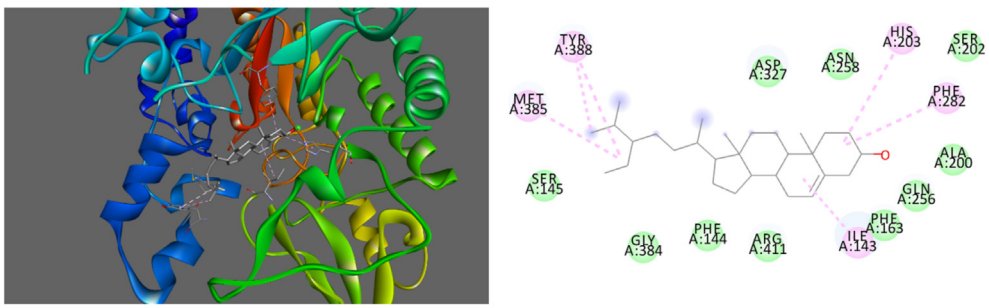


**Figure 2.** 3D (left) and 2D (right) visualizations of the interactions between β-sitosterol and AG.

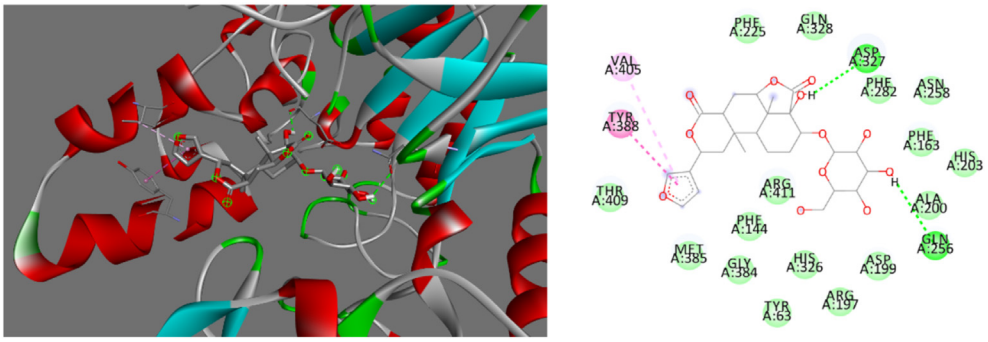


**Figure 3.** 3D (left) and 2D (right) visualizations of the interactions between borapetoside A and AG.

**Table 9.** Chemical interaction analyses of the inhibitory activity of borapetoside A against AG using Discovery Studio.

| Receptor (amino acid) | Distance (Å) | Ligand (group) | Receptor (group) | Chemical interaction |
|---|---|---|---|---|
| ASP327 | 2.30238 | H-Donor | H-Acceptor | Hydrogen bond |
| GLN256 | 3.04358 | H-Donor | H-Acceptor | Hydrogen bond |
| TYR388 | 5.29125 | Pi-Orbitals | Pi-Orbitals | Hydrophobic |
| VAL405 | 5.4311 | Pi-Orbitals | Alkyl | Hydrophobic |

The plants were extracted by infusion with 70% ethanol, sonicated with a 50 KHz ultrasound machine for 30 min, and then filtered. To increase the yield, the ultrasonication step was repeated twice. Finally, the extract was evaporated and dried with a rotary evaporator. The dry extract was weighed and stored at 4 °C *prior* to further testing.

### 2.3. AG inhibition test

Stock solutions of Thai herbal recipe extracts, including *A. paniculate*, *T. crispa*, *S. suberosa*, *T. laurifolia*, and *C. verum,* were prepared at a concentration of 8 mg/mL in dimethyl sulfoxide (DMSO). AG inhibition was determined for all extracts according to previously reported assays [43]. Briefly, p-nitrophenol (yellow in color), which was released from p-nitrophenyl-alpha-D-glucopyranoside (pNPG), was detected by measuring the absorbance at 405 nm. The samples were prepared at a concentration of 8 mg/mL and consisted of 50 μL of sample solution mixed with 50 μL of phosphate-buffered saline (PBS) containing 2 mg/mL bovine serum albumin, 0.2 mg/mL sodium azide and 50 μL of 1 unit/mL AG. DMSO (5%) and acabose [44] were used as negative and positive controls, respectively. All plates were placed in an incubator under a controlled environment of 37 °C for 2 min. Then, 4 mM pNPG was added to each well. The reaction was monitored with a microplate reader at 405 nm every 5 min for a total of 6 measurements. The percent inhibition of AG was calculated according to Eq. (3). The results are reported as the 50% inhibition of AG activity ($IC_{50}$).

$$AG\ inhibition\ rate\ (\%) = \left(1 - \frac{OD_{sample} - OD_{blank}}{OD_{control} - OD_{blank}}\right) x\ 100 \quad (3)$$

### 2.4. Molecular docking and chemical visualization

Targeted protein-specified ligand dockings were prepared to verify whether a ligand was a better inhibitor of AG than acabose (PDB 5ZCC), which is the standard diabetes treatment. The inhibition of AG has been studied in the five plants used for the treatment of diabetes. Twenty-one compounds derived from *A. paniculate* [45, 46, 47, 48, 49], 16 compounds derived from *C. verum* [50, 51, 52], 11 compounds derived from *S. suberosa* [53, 54], 9 compounds derived from *T. crispa* L [55, 56, 57], and 4 compounds derived from *T. laurifolia* [58, 59] were docked into the AG target site AG with ArgusLab. Docking effects were considered when the binding energy values were less than those of acabose-AG. AutoDock

**Table 10.** Chemical interaction analyses of the inhibitory activity of borapetoside D against AG using Discovery Studio.

| Receptor (amino acid) | Distance (Å) | Ligand (group) | Receptor (group) | Chemical interaction |
|---|---|---|---|---|
| ASP382 | 2.33377 | H-Donor | H-Acceptor | Hydrogen bond |
| ASP327 | 3.08067 | H-Donor | H-Acceptor | Hydrogen bond |
| ARG411 | 3.1259 | H-Acceptor | H-Donor | Hydrogen bond |
| MET285 | 3.43083 | H-Donor | H-Acceptor | Hydrogen bond |
| ASP382 | 3.54343 | H-Donor | H-Acceptor | Hydrogen bond |
| PHE144 | 3.58219 | H-Acceptor | H-Donor | Hydrogen bond |
| GLY384 | 3.56044 | H-Acceptor | H-Donor | Hydrogen bond |
| MET285 | 3.82702 | Pi-Orbitals | Amide | Hydrophobic |
| ILE143 | 4.59271 | Alkyl | Alkyl | Hydrophobic |

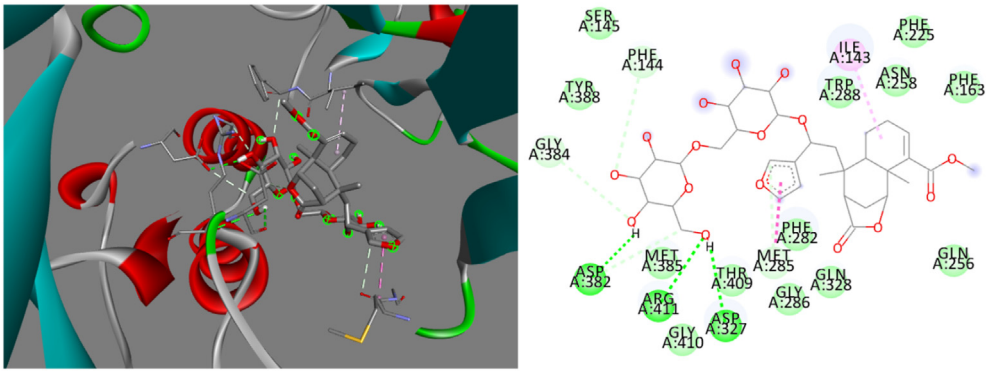


**Figure 4.** 3D (left) and 2D (right) visualizations of the interactions between borapetoside D and AG.

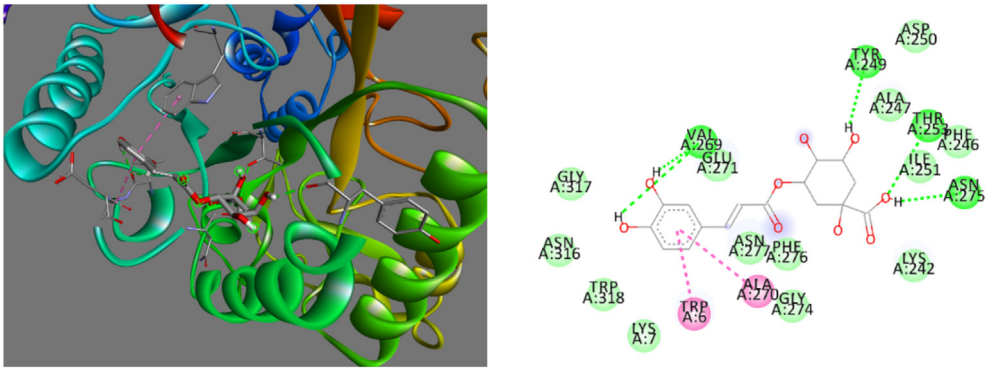


**Figure 5.** 3D (left) and 2D (right) visualizations of the interactions between chlorogenic acid and AG.

**Table 11.** Chemical interaction analyses of the inhibitory activity of chlorogenic acid against AG using Discovery Studio.

| Receptor (amino acid) | Distance (Å) | Ligand (group) | Receptor (group) | Chemical interaction |
|---|---|---|---|---|
| VAL269 | 2.52232 | H-Donor | H-Acceptor | Hydrogen bond |
| VAL269 | 2.09319 | H-Donor | H-Acceptor | Hydrogen bond |
| TYR249 | 2.16522 | H-Donor | H-Acceptor | Hydrogen bond |
| THR253 | 2.97136 | H-Acceptor | H-Donor | Hydrogen bond |
| ASN275 | 2.30895 | H-Donor | H-Acceptor | Hydrogen bond |
| ALA270 | 4.68184 | Pi-Orbitals | Amide | Hydrophobic |
| TRP6 | 4.76658 | Pi-Orbitals | Pi-Orbitals | Hydrophobic |

Vina was used to verify the top binding value, and the following parameters were set to calculate the binding energies: the selected box size was x = 62, y = 60, z = 84; the box position was x = 4.016, y = 49.080, z = 82.173; and the exhaustiveness number was set to 20. In addition, AutoDock was used to confirm the binding affinity with the same box settings as those used for AutoDock Vina, and the 50% inhibition constant ($IC_{50}$) was predicted by Eq. (4)

$$\text{Inhibition constant}\left(K_i\right) = \frac{IC50}{(1 + ([L]/Kd)} \quad (4)$$

where.

$K_i$ is the inhibition constant, which was calculated from $K_i = \exp(\Delta G/R \times T)$,
$K_d$ is the dissociation constant, and
L is the ligand concentration.

The chemical interactions (hydrogen bonds and hydrophobic interactions) between the best-binding ligand and the target protein pocket site were visualized with Discovery Studio.

### 2.5. Pharmacokinetics prediction

The pharmacokinetic parameters of the compounds with the best binding were investigated using SwissADME. This tool was used to predict GI absorption and brain access in a representative region of the BOILED-Egg construction. There are 2 BOILED-Egg regions, as follows: the white region of the model indicates that the compounds are absorbed well by the GI tract and the yellow region of the model indicates that the compounds permeate the brain. A blue color indicates that the compound is effluated from the central nervous system (CNS) and vice versa for a red color.

**Table 12.** Chemical interaction analyses of the inhibitory activity of ergosterol peroxide against AG using Discovery Studio.

| Receptor (amino acid) | Distance (Å) | Ligand (group) | Receptor (group) | Chemical interaction |
|---|---|---|---|---|
| MET385 | 4.99848 | Alkyl | Alkyl | Hydrophobic |
| PHE163 | 5.25594 | Alkyl | Pi-Orbitals | Hydrophobic |
| ILE143 | 4.69368 | Alkyl | Alkyl | Hydrophobic |
| TYR63 | 3.78582 | C–H | Pi-Orbitals | Hydrophobic |
| TYR63 | 3.99026 | C–H | Pi-Orbitals | Hydrophobic |
| PHE163 | 3.99593 | C–H | Pi-Orbitals | Hydrophobic |

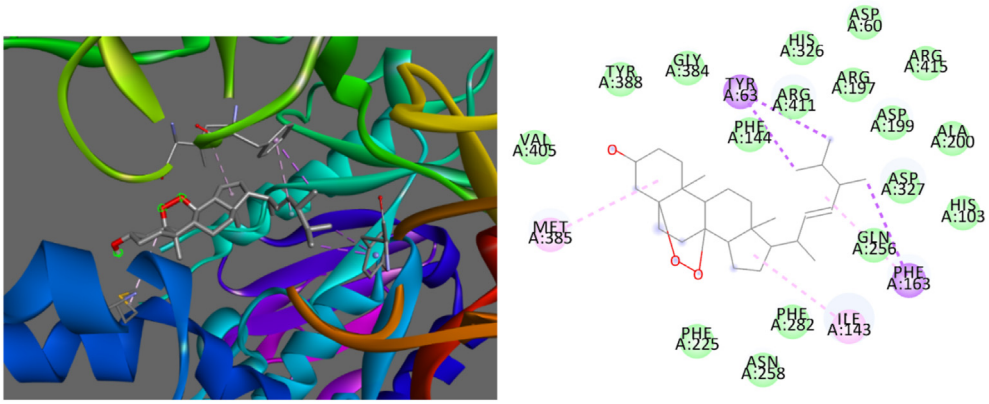


**Figure 6.** 3D (left) and 2D (right) visualizations of the interactions between ergosterol peroxide and AG.

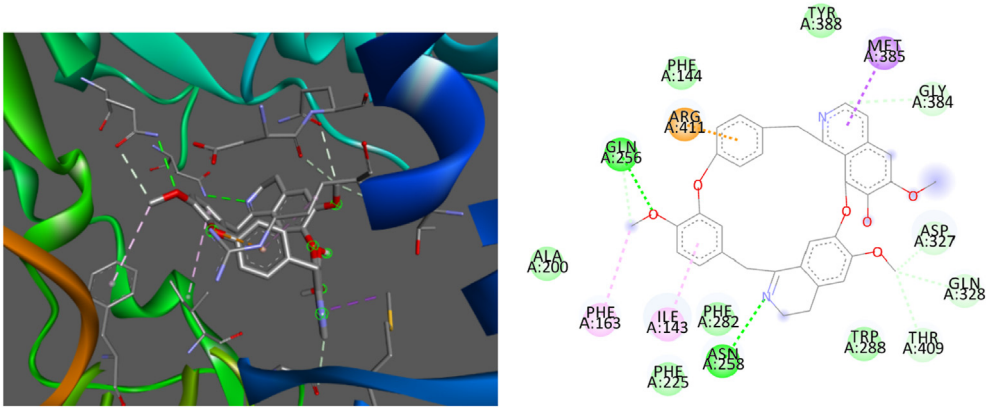


**Figure 7.** 3D (left) and 2D (right) visualizations of the interactions between stephasubimine and AG.

**Table 13.** Chemical interaction analyses of the inhibitory activity of stephasubimine against AG using Discovery Studio.

| Receptor (amino acid) | Distance (Å) | Ligand (group) | Receptor (group) | Chemical interaction |
|---|---|---|---|---|
| MET385 | 4.99848 | Alkyl | Alkyl | Hydrophobic |
| PHE163 | 5.25594 | Alkyl | Pi-Orbitals | Hydrophobic |
| ILE143 | 4.69368 | Alkyl | Alkyl | Hydrophobic |
| TYR63 | 3.78582 | C–H | Pi-Orbitals | Hydrophobic |
| TYR63 | 3.99026 | C–H | Pi-Orbitals | Hydrophobic |
| PHE163 | 3.99593 | C–H | Pi-Orbitals | Hydrophobic |

### 2.6. Solvent considerations for selected compounds

To enhance the extraction yields of specific compounds, COSMOquick was used to screen which solvents were suitable for extraction [60]. Six compounds were evaluated in six different solvents, including water, ethanol, methanol, chloroform, acetone, and tetrahydrofuran (THF). The solvents were characterized according to their physical and chemical parameters, such as their solubility, dielectric constant and donor and acceptor properties. In this study, four parameters were considered for the selected compounds, including $\Delta H_{fus}$, T (set to room temperature), and the $T_m$ of the compound. Thus, the solubility of the selected compounds in different solvents could be predicted computationally using the COSMOquick mathematical software approach following Eq. (5).

$$\Delta G_{fus} = \Delta H_{fus} - \Delta H_{fus}\,(1-T)/T_m \quad (5)$$

### 2.7. Statistical analysis

All statistical analyses were conducted using one-way ANOVA. The results were analyzed by the SPSS 18 software with Tukey's comparison test for comparisons between compounds. Differences were considered statistically significant when the *p*-value was less than 0.05 (*), 0.01 (**), 0.005 (***), and 0.001 (****). All values are presented as the mean ± standard deviation (SD).

## 3. Results and discussion

### 3.1. AG inhibition test

The in vitro AG inhibitory activity assay results showed that the 5 selected Thai herbs inhibited AG. Figure 1 shows that the *C. verum* extract (CV) ($IC_{50} = 0.35 \pm 0.12$ mg/mL) possessed the strongest inhibition with the lowest yield extraction (14.4%), followed by the *T. crispa* extract (TC)

**Table 14.** Chemical interaction analyses of the inhibitory activity of stephasubine against AG using Discovery Studio.

| Receptor (amino acid) | Distance (Å) | Ligand (group) | Receptor (group) | Chemical interaction |
|---|---|---|---|---|
| ASN258 | 3.23635 | H-Acceptor | H-Donor | Hydrogen bond |
| MET285 | 3.42259 | H-Donor | H-Acceptor | Hydrogen bond |
| ASP327 | 3.49748 | H-Donor | H-Acceptor | Hydrogen bond |
| PHE282 | 5.31555 | Pi-Orbitals | Pi-Orbitals | Hydrophobic |
| MET385 | 4.76705 | Alkyl | Alkyl | Hydrophobic |
| ARG411 | 3.90756 | Alkyl | Alkyl | Hydrophobic |
| TRP288 | 5.45615 | Pi-Orbitals | Pi-Orbitals | Hydrophobic |

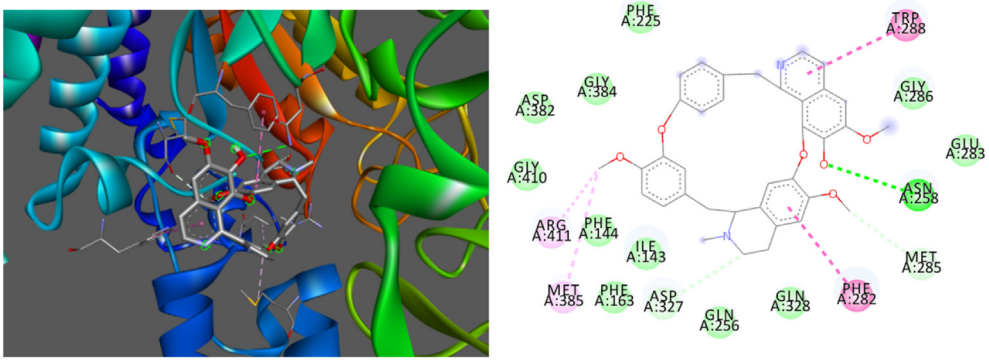


**Figure 8.** 3D (left) and 2D (right) visualizations of the interactions between stephasubine and AG.

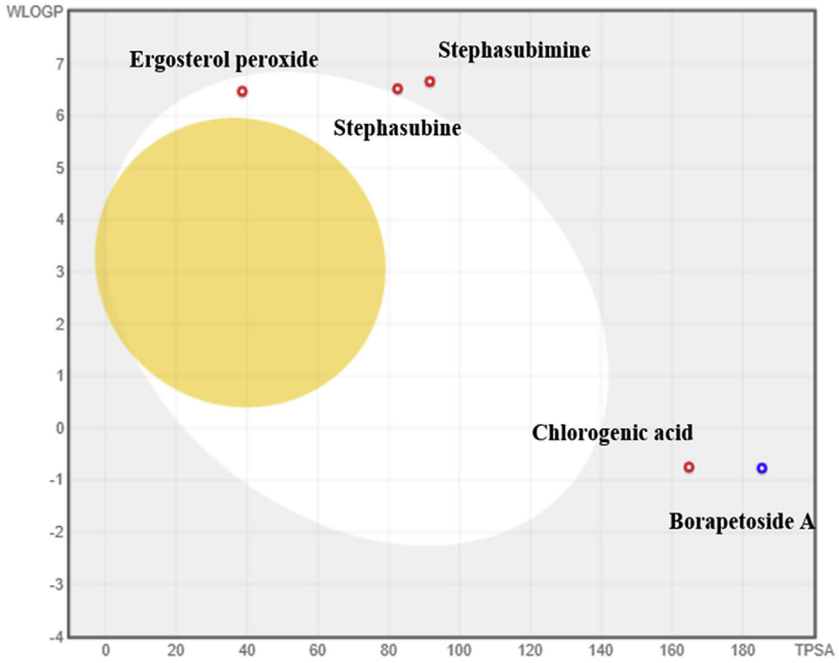


**Figure 9.** BOILED-Egg model of selected top-ranking compounds from the docking study.

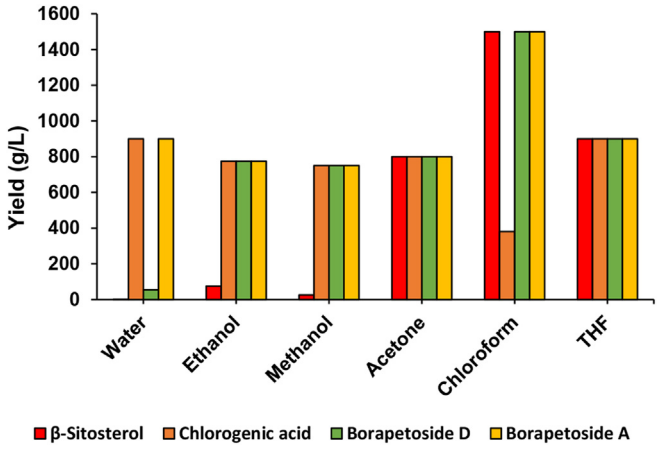


**Figure 10.** Correlations between extraction with various solvents and the corresponding yield.

($IC_{50}$ = 0.69 ± 0.39 mg/mL) with an extraction yield of 9.6%, the *S. suberosa* extract (SS) ($IC_{50}$ = 1.5 ± 0.17 mg/mL) with an extraction yield of 8.7%, the *A. paniculate* extract (AP) ($IC_{50}$ = 1.78 ± 0.35) with an extraction yield of 10.7% and the *T. laurifolia* extract (Tl) ($IC_{50}$ = 4.66 ± 0.27 mg/mL) with an extraction yield of 11.2%. In addition, the improvement of this Thai recipe extracted with chloroform demonstrated that the AG inhibition properties of this recipe were more effective (Table 1) because the main compounds, such as boraptoside A and boraptoside D from *T. crispa*, can be extracted in chloroform with the highest yields, meaning that the *T. crispa* chloroform extraction is able to inhibit the enzyme better than the water extraction. However, it was found that the chlorogenic compound from *C. verum* was good when extracted with water. It was able to inhibit AG enzymes better than the chloroform extraction because chlorogenic compounds are more soluble in water than in chloroform. The extraction of this herbal recipe with chloroform was compared to that extracted with water and alcohol. The recipe extracted in chloroform had a stronger inhibitory effect than those extracted with water and ethanol because the main active compounds that inhibit AG enzymes can be extracted with chloroform in the highest yields when compared to water and alcohol extraction.

### 3.2. Molecular docking

To develop an herbal extract with the highest inhibitory activity against AG, the binding affinities of the compounds derived from each herb were evaluated. Among the 61 compounds, the top 7 compounds strongly inhibited AG compared to acarbose, as shown in Tables 1, 2, 3, 4, 5, and 6. These top 7 compounds were β-sitosterol, ergosterol peroxide, chlorogenic acid, borapetoside D, borapetoside A, stephasubine, and stephasubimine. The minimum binding energy of β-sitosterol with AG after examination by ArgusLab, AutoDock Vina, and AutoDock was found to be -14.0, -8.2, and -11.4 kcal/mol, respectively. The minimum binding energy of ergosterol peroxide with AG after evaluation with ArgusLab, AutoDock Vina, and AutoDock was found to be -10.1, -9.6, and -11.4 kcal/mol, respectively. The minimum binding energy of chlorogenic acid with AG after evaluation by ArgusLab, AutoDock Vina, and AutoDock was found to be -10.7, -8.1, and -12.4 kcal/mol, respectively. The minimum binding energy of borapetoside D with AG after evaluation by ArgusLab, AutoDock Vina, and AutoDock was found to be -9.7, -8.2, and -12.7 kcal/mol, respectively. The minimum binding energy of borapetoside A with AG after evaluation by ArgusLab, AutoDock Vina, and AutoDock was found to be -9.1, -9.2, and -12.2 kcal/mol, respectively. The minimum binding energy of stephasubine with AG after evaluation by ArgusLab, AutoDock Vina, and AutoDock was found to be -9.1, -9.0, and -12.6 kcal/mol, respectively. Finally, the minimum binding energy of stephasubimine with AG after evaluation by ArgusLab, AutoDock Vina, and AutoDock was found to be -8.3, -9.7, and -13.0 kcal/mol, respectively. Thus, the inhibition constants of β-sitosterol, ergosterol peroxide, borapetoside A, chlorogenic acid, stephasubine, borapetoside D, and stephasubimine were calculated from the minimum binding energies to be 4.46 nM, 4.18 nM, 1.09 nM, 819.07 pM, 560.6 pM, 508.63 pM, and 285.37 pM, respectively. The minimum binding energy of acabose with AG after evaluation by ArgusLab, AutoDock Vina, and AutoDock was -7.6, -8.1, and -9.1 kcal/mol, respectively, and the inhibition constant was determined to be 212.84 nM.

### 3.3. Visualization of the ligands and receptor

The chemical interactions between each compound and the protein were visualized and represented by H-bonding and hydrophobic interactions. The results revealed that these top selected compounds bind to different pocket sites in AG, which indicated the potential for greater inhibition by a combination of compounds than by the use of a single compound. According to Tables 3, 4, 5, 6, and 7, there were 7 compound-AG complexes, as follows: β-sitosterol-AG, ergosterol peroxide-AG, chlorogenic acid-AG, borapetoside D-AG, borapetoside A-AG, stephasubine-AG, and stephasubimine-AG, each of which displayed a binding energy that was less than that of acabose (positive control).

Based on the binding energies and different pocket binding sites of the selected compounds with AG, these seven compounds possessed low binding energies to AG that were superior to that of acabose. The chemical binding interactions between these compounds and the targeted protein were visualized by Discovery Studio. To determine the best conformation of each compound for AG inhibition, the binding sites of AG with these 7 compounds were clarified. β-Sitosterol strongly bound to MET385, ILE143, HIS203, PHE282, and TYR388 of AG, as shown in Figure 2. The interactions of β-sitosterol with AG were hydrophobic, as shown in Table 8. Borapetoside A strongly interacted with ASP327, GLN256, TYR388, and VAL405, as shown in Figure 3. Borapetoside A interacted with AG via hydrogen bonding and hydrophobic interactions, as shown in Table 9. Borapetoside D strongly bound to ASP382, ASP327, ARG411, MET285, ASP382, PHE144, GLY384, MET285, and ILE143, as shown in Figure 4. The interactions of borapetoside D with AG occurred via hydrogen bonding and hydrophobic interactions, as shown in Table 10. Chlorogenic acid strongly interacted with VAL269, TYR249, THR253, ASN275, ALA270, and TRP6, as shown in Figure 5. The interactions of chlorogenic acid with AG occurred via hydrogen bonding and hydrophobic interactions, as shown in Table 11. Ergosterol peroxide strongly bound to MET385, PHE163, ILE143, and TYR63, as shown in Figure 6. The interactions of ergosterol peroxide with AG were hydrophobic, as shown in Table 12. Stephasubimine strongly interacted with MET385, PHE163, ILE143, and TYR63, as shown in Figure 7. The interactions of stephasubimine with AG were hydrophobic, as shown in Table 13. Stephasubine strongly bound to ASN258, MET285, ASP327, PHE282, MET385, ARG411, and TRP288, as shown in Figure 8. The interactions of stephasubine with AG occurred via hydrogen bonding and hydrophobic interactions, as shown in Table 14. These 7 selected compounds from 3 herbs are promising compounds to replace acabose. However, these compounds should be studied regarding their extraction from the herbs and their pharmacokinetics after administration.

### 3.4. Pharmacokinetics

The seven top-ranking compounds from the docking analyses were analyzed for their absorption, distribution, metabolism and excretion (ADME) properties, as shown in Figure 9. To select the best compounds for inhibition against AG in the human body, this study considered low absorption through the GI tract. The compounds should competitively bind to AG prior to binding carbohydrates to inhibit the conversion of carbohydrates into glucose. Therefore, compounds with a high binding affinity and low absorption in the GI tract were selected as candidates for development into antidiabetic compounds. The dots located outside the yellow and white regions of the BOILED-Egg model were considered. Among the seven compounds, six compounds (β-sitosterol, chlorogenic acid, borapetoside D, borapetoside A, stephasubine, and stephasubimine, but not ergosterol peroxide) exhibited low absorption in the GI tract.

### 3.5. Solvent considerations for the selected compounds

The optimum solubilities of the selected compounds were calculated by Eq. (3). As shown in Figure 10, the maximum extraction of β-sitosterol, borapetoside D, and borapetoside A occurred in chloroform. The extraction of chlorogenic acid showed the highest yield with water. A previous study suggested dichloromethane and chloroform for the extraction of stephasubine and stephasubimine [61, 62].

## 4. Conclusions

Although the studied Thai remedy has been used to treat diabetes for a long time and has shown good results, there is still a lack of scientific proof of the mechanisms of its efficacy. After an *in vitro* study of the crude herbal extracts, it was found that the inhibitory activities of these crude extracts against AG were lower than that of acabose. Except for the inhibitory activity of the *T. crispa* and *C. verum* extracts, the efficacy of the extracts was not different from that of acabose. Therefore, to overcome this limitation, it was necessary to improve the efficacy of this Thai remedy via docking analysis. This study showed that six active compounds, namely, β-sitosterol, chlorogenic acid, borapetoside D, borapetoside A, stephasubine, and stephasubimine, more strongly inhibited AG than acabose and exhibited low bioavailability. Moreover, to enhance the extraction yield of each compound, the choice of solvent must be considered. To enhance the yield of β-sitosterol, the solvent calculations suggested that *A. paniculate* should be extracted with chloroform. For chlorogenic acid, the suggested solvent for extraction from *C. verum* was water. For borapetoside D and borapetoside A, the suggested solvent for extraction from *T. crispa* was chloroform. To provide optimum yields of stephasubine and stephasubimine, the suggested solvent for extraction from *S. suberosa* was dichloromethane. Thus, it was found that six active compounds derived from three herbs and extracted by different specific solvents were suitable for the development of this recipe and could be more effective than acabose in decreasing glucose levels. According to computer prediction results and confirmed by in vitro experiments, this recipe extracted with chloroform has a stronger inhibitory effect than the water and ethanol extractions because the main active compounds that have the ability to inhibit AG enzymes can be extracted with chloroform in the highest yields when compared to water and alcohol.

## Declarations

### Author contribution statement

Komgrit Eawsakul: Conceived and designed the experiments; Performed the experiments; Analyzed and interpreted the data; Contributed reagents, materials, analysis tools or data; Wrote the paper.

Pharkphoom Panichayupakaranant: Conceived and designed the experiments; Wrote the paper.

Tassanee Ongtanasup: Analyzed and interpreted the data; Wrote the paper.

Sakan Warinhomhoun: Performed the experiments; Analyzed and interpreted the data.

Kunwadee Noonong: Performed the experiments; Contributed reagents, materials, analysis tools or data.

Kingkan Bunluepuech: Conceived and designed the experiments; Analyzed and interpreted the data; Wrote the paper.

### Funding statement

This work was partially supported by the New Strategic Research (P2P) project, Walailak University, Thailand and partially supported by Prince of Songkla University, Thailand (no. TTM580909s).

### Data availability statement

Data will be made available on request.

### Declaration of interests statement

The authors declare no conflict of interest.

## Additional information

No additional information is available for this paper.

## Acknowledgements

We would like to thank the Center of Excellence Research for Innovation and Health Product and the School of Medicine, Walailak University for providing the equipment.

## References

[1] K. Ogurtsova, J. da Rocha Fernandes, Y. Huang, et al., IDF Diabetes Atlas: global estimates for the prevalence of diabetes for 2015 and 2040, Diabetes Res. Clin. Pract. 128 (2017) 40–50.
[2] A. Vas, E.S. Devi, S. Vidyasagar, et al., Effectiveness of self-management programmes in diabetes management: a systematic review, Int. J. Nurs. Pract. 23 (5) (2017), e12571.
[3] J.E. Reusch, J.E. Manson, Management of type 2 diabetes in 2017: getting to goal, JAMA 317 (10) (2017) 1015–1016.
[4] S. Davoudi, L. Sobrin, Novel genetic actors of diabetes-associated microvascular complications: retinopathy, kidney disease and neuropathy, Reg. Dev. Stud. 12 (3-4) (2015) 243.
[5] Y.-T. Deng, S.-Y. Lin-Shiau, L.-F. Shyur, J.-K. Lin, Pu-erh tea polysaccharides decrease blood sugar by inhibition of α-glucosidase activity in vitro and in mice, Food Funct. 6 (5) (2015) 1539–1546.
[6] T. Satoh, M. Igarashi, S. Yamada, N. Takahashi, K.J. Watanabe, Inhibitory effect of black tea and its combination with acarbose on small intestinal α-glucosidase activity, J. Ethnopharmacol. 161 (2015) 147–155.
[7] R. Ortiz-Andrade, S. Garcia-Jimenez, P. Castillo-Espana, G. Ramirez-Avila, R. Villalobos-Molina, S.J. Estrada-Soto, α-Glucosidase inhibitory activity of the methanolic extract from Tournefortia hartwegiana: an anti-hyperglycemic agent, J. Ethnopharmacol. 109 (1) (2007) 48–53.
[8] K.J. Zerr, A.P. Furnary, G.L. Grunkemeier, S. Bookin, V. Kanhere, A. Starr, Glucose control lowers the risk of wound infection in diabetics after open heart operations, Ann. Thorac. Surg. 63 (2) (1997) 356–361.
[9] S. Kumar, S. Narwal, V. Kumar, O. Prakash, α-glucosidase inhibitors from plants: a natural approach to treat diabetes, Phcog. Rev. 5 (9) (2011) 19.
[10] H. Matsuura, C. Asakawa, M. Kurimoto, J. Mizutani, α-glucosidase inhibitor from the seeds of balsam pear (Momordica charantia) and the fruit bodies of Grifola frondosa, Biosci. Biotechnol. Biochem. 66 (7) (2002) 1576–1578.
[11] Y.-M. Kim, Y.-K. Jeong, M.-H. Wang, W.-Y. Lee, H.-I. Rhee, Inhibitory effect of pine extract on α-glucosidase activity and postprandial hyperglycemia, Nutrition 21 (6) (2005) 756–761.
[12] X. Zhang, Z. Fang, C. Zhang, et al., Effects of acarbose on the gut microbiota of prediabetic patients: a randomized, double-blind, controlled crossover trial, Diabetes Therap. 8 (2) (2017) 293–307.
[13] W. Wutthithammavet, Herbal Encyclopaedia, Odeanstore press, Bangkok, 1997.
[14] R. Subramanian, M.Z. Asmawi, A. Sadikun, In vitro alpha-glucosidase and alpha-amylase enzyme inhibitory effects of Andrographis paniculata extract and andrographolide, Acta Biochim. Pol. 55 (2) (2008) 391–398.
[15] R. Subramanian, M.Z. Asmawi, Inhibition of α-Glucosidase by Andrographis paniculata. Ethanol extract in rats, Pharmaceut. Biol. 44 (8) (2006) 600–606.
[16] X.F. Zhang, B.K. Tan, Antihyperglycaemic and anti-oxidant properties of andrographis paniculata in normal and diabetic rats, Clin. Exp. Pharmacol. Physiol. 27 (5-6) (2000) 358–363.
[17] C. Calabrese, S.H. Berman, J.G. Babish, et al., A phase I trial of andrographolide in HIV positive patients and normal volunteers, Phytother Res. 14 (5) (2000) 333–338.
[18] Y.C. Shen, C.F. Chen, W.F. Chiou, Andrographolide prevents oxygen radical production by human neutrophils: possible mechanism (s) involved in its anti-inflammatory effect, Br. J. Pharmacol. 135 (2) (2002) 399–406.
[19] P. Misra, N. Pal, P. Guru, J. Katiyar, V. Srivastava, J.S. Tandon, Antimalarial activity of andrographis paniculata (Kalmegh) against plasmodium berghei NK 65 in mastomys natalensis, Int. J. Pharmacogn. 30 (4) (1992) 263–274.
[20] D. See, S. Mason, R. Roshan, Increased tumor necrosis factor alpha (TNF-α) and natural killer cell (NK) function using an integrative approach in late stage cancers, Immunol. Invest. 31 (2) (2002) 137–153.
[21] A. Kapil, I.B. Koul, S.K. Banerjee, B.D. Gupta, Antihepatotoxic effects of major diterpenoid constituents of Andrographis paniculata, Biochem. Pharmacol. 46 (1) (1993) 182–185.
[22] H. Zhao, W.J. Fang, Antithrombotic effects of Andrographis paniculata nees in preventing myocardial infarction, Chin. Med. J. 104 (9) (1991) 770–775.
[23] T. Matsuda, M. Kuroyanagi, S. Sugiyama, et al., Cell differentiation-inducing diterpenes from Andrographis paniculata Nees, Chem. Pharm. Bull. 42 (6) (1994) 1216–1225.
[24] E.W. Chan, S.Y. Eng, Y.P. Tan, Z.C. Wong, Phytochemistry and pharmacological properties of Thunbergia laurifolia: a Review, Phcog. J. 3 (24) (2011) 1–6.
[25] M. Junsi, S. Siripongvutikorn, Thunbergia laurifolia, a traditional herbal tea of Thailand: botanical, chemical composition, biological properties and processing influence, Int. Food Res. J. 23 (3) (2016) 923.
[26] J.D. Gimlette, I.H. Burkill, The Medical Book of Malayan Medecine, Verlag nicht ermittelbar, 1930.
[27] H. Noor, P. Hammonds, R. Sutton, S.J.D. Ashcroft, The hypoglycaemic and insulinotropic activity of Tinospora crispa: studies with human and rat islets and HIT-T15 B cells, Diabetologia 32 (6) (1989) 354–359.
[28] R.S. Gupta, J.J. Krepinsky, L. Siminovitch, Structural determinants responsible for the biological activity of (-)-emetine,(-)-cryptopleurine, and (-)-tylocrebrine: structure-activity relationship among related compounds, Pharmacology 18 (1) (1980) 136–143.
[29] L. Jiao, X. Zhang, L. Huang, et al., Proanthocyanidins are the major anti-diabetic components of cinnamon water extract, Food Chem. Toxicol. 56 (2013) 398–405.
[30] D.M. Cheng, P. Kuhn, A. Poulev, L.E. Rojo, M.A. Lila, I.J.F.c. Raskin, In vivo and in vitro antidiabetic effects of aqueous cinnamon extract and cinnamon polyphenol-enhanced food matrix, Food Chem. 135 (4) (2012) 2994–3002.
[31] P. Crawford, Effectiveness of cinnamon for lowering hemoglobin A1C in patients with type 2 diabetes: a randomized, controlled trial, J. Am. Board Fam. Med. 22 (5) (2009) 507–512.
[32] P. Tangyuenyongwatana, N. Jongkon, Molecular docking study of tyrosinase inhibitors using ArgusLab 4.0. 1: a comparative study, Thai J. Pharmaceut. Sci. 40 (1) (2016).
[33] G. Bitencourt-Ferreira, W.F. de Azevedo, Molecular docking simulations with ArgusLab. Docking Screens for Drug Discovery, 2019, pp. 203–220.
[34] I. Ali, R. Rafique, K.M. Khan, et al., Potent α-amylase inhibitors and radical (DPPH and ABTS) scavengers based on benzofuran-2-yl (phenyl) methanone derivatives: syntheses, in vitro, kinetics, and in silico studies, Bioorg. Chem. 104 (2020) 104238.
[35] M. Solangi, K.M. Khan, F. Saleem, et al., Indole acrylonitriles as potential anti-hyperglycemic agents: synthesis, α-glucosidase inhibitory activity and molecular docking studies, Bioorg. Med. Chem. 28 (21) (2020) 115605.
[36] F. Rahim, M. Taha, N. Iqbal, et al., Isatin based thiosemicarbazide derivatives as potential inhibitor of α-glucosidase, synthesis and their molecular docking study, J. Mol. Struct. 1222 (2020) 128922.
[37] M.A. Rauf, S. Zubair, A. Azhar, Ligand docking and binding site analysis with pymol and autodock/vina, J. Comput. Aided Mol. Des. 4 (2) (2015) 168.
[38] A. Daina, V.J.C. Zoete, A boiled-egg to predict gastrointestinal absorption and brain penetration of small molecules, ChemMedChem 11 (11) (2016) 1117.
[39] A.R. Katritzky, M. Kuanar, S. Slavov, et al., Quantitative correlation of physical and chemical properties with chemical structure: utility for prediction, Chem. Rev. 110 (10) (2010) 5714–5789.
[40] P. Kolář, J.-W. Shen, A. Tsuboi, T. Ishikawa, Solvent selection for pharmaceuticals, Fluid Phase Equil. 194 (2002) 771–782.
[41] C. Spickermann, J. Thar, S. Lehmann, et al., Why are ionic liquid ions mainly associated in water? A Car–Parrinello study of 1-ethyl-3-methyl-imidazolium chloride water mixture, J. Chem. Phys. 129 (10) (2008) 104505.
[42] A. Niederquell, N. Wyttenbach, M. Kuentz, New prediction methods for solubility parameters based on molecular sigma profiles using pharmaceutical materials, Int. J. Pharm. 546 (1-2) (2018) 137–144.
[43] S. Dej-adisai, T. Pitakbut, C. Wattanapiromsakul, Alpha-glucosidase inhibitory activity and phytochemical investigation of Borassus flabellifer Linn, Afr. J. Pharm. Pharmacol. 11 (3) (2017) 45–52.
[44] M. Nawaz, M. Taha, F. Qureshi, et al., Structural elucidation, molecular docking, α-amylase and α-glucosidase inhibition studies of 5-amino-nicotinic acid derivatives, BMC Chem. 14 (1) (2020) 1–11.
[45] D.C. Jain, M.M. Gupta, S. Saxena, S. Kumar, LC analysis of hepatoprotective diterpenoids from Andrographis paniculata, J. Pharmaceut. Biomed. Anal. 22 (4) (2000) 705–709.
[46] M.K. Reddy, M.V. Reddy, D. Gunasekar, M.M. Murthy, C. Caux, B.J.P. Bodo, A flavone and an unusual 23-carbon terpenoid from Andrographis paniculata, Phytochemistry 62 (8) (2003) 1271–1275.
[47] Y.K. Rao, G. Vimalamma, C.V. Rao, Y.-M. Tzeng, Flavonoids and andrographolides from Andrographis paniculata, Phytochemistry 65 (16) (2004) 2317–2321.
[48] C. Xu, G.X. Chou, Z.T. Wang, A new diterpene from the leaves of Andrographis paniculata Nees, Fitoterapia 81 (6) (2010) 610–613.
[49] W.-W. Chao, B.-F. Lin, Isolation and identification of bioactive compounds in Andrographis paniculata (Chuanxinlian), Chin. Med. 5 (1) (2010) 17.
[50] S.Y. Subki, J.A. Jamal, K. Husain, N. Manshoor, Characterisation of leaf essential oils of three Cinnamomum species from Malaysia by gas chromatography and multivariate data analysis, Phcog. J. 5 (1) (2013) 22–29.
[51] K.N.S. Kumar, B. Sangeetha, M. Rajalekshmi, B. Ravishankar, R. Muralidhar, B. Yashovarma, Chemoprofile of tvakpatra; leaves of Cinnamomum verum JS Presl, Phcog. J. 4 (34) (2012) 26–30.
[52] G.E.-S. Batiha, A.M. Beshbishy, A. Guswanto, et al., Phytochemical characterization and chemotherapeutic potential of Cinnamomum verum extracts on the multiplication of protozoan parasites in vitro and in vivo, Molecules 25 (4) (2020) 996.
[53] A. Patra, C.T. Montgomery, A.J. Freyer, et al., The protoberberine alkaloids of Stephania suberosa, Phytochemistry 26 (2) (1987) 547–549.
[54] D.K. Semwal, R. Badoni, R. Semwal, S.K. Kothiyal, G.J.P. Singh, U. Rawat, The genus Stephania (Menispermaceae): chemical and pharmacological perspectives, J. Ethnopharmacol. 132 (2) (2010) 369–383.
[55] C.-T. Ruan, S.-H. Lam, T.-C. Chi, S.-S. Lee, M.-J. Su, Borapetoside C from Tinospora crispa improves insulin sensitivity in diabetic mice, Phytomedicine 19 (8-9) (2012) 719–724.
[56] S. Praman, M.J. Mulvany, D.E. Williams, R.J. Andersen, C. Jansakul, Hypotensive and cardio-chronotropic constituents of Tinospora crispa and mechanisms of action

on the cardiovascular system in anesthetized rats, J. Ethnopharmacol. 140 (1) (2012) 166–178.
[57] F.E. Lokman, H.F. Gu, W.N. Wan Mohamud, et al., Antidiabetic effect of oral borapetol B compound, isolated from the plant Tinospora crispa, by stimulating insulin release, Evid. base Compl. Alternative Med. 2013 (2013).
[58] T. Kanchanapoom, R. Kasai, K.J.P. Yamasaki, Iridoid glucosides from Thunbergia laurifolia, Phytochemistry 60 (8) (2002) 769–771.
[59] R. Oonsivilai, C. Cheng, J. Bomser, M.G. Ferruzzi, S. Ningsanond, Phytochemical profiling and phase II enzyme-inducing properties of Thunbergia laurifolia Lindl.(RC) extracts, J. Ethnopharmacol. 114 (3) (2007) 300–306.
[60] R. Van Kerrebroeck, P. Naert, T.S. Heugebaert, M. D'hooghe, C.V. Stevens, Electrophilic bromination in flow: a safe and sustainable alternative to the use of molecular bromine in batch, Molecules 24 (11) (2019) 2116.
[61] A. Zahari, A. Ablat, Y. Sivasothy, J. Mohamad, M.I. Choudhary, K. Awang, In vitro antiplasmodial and antioxidant activities of bisbenzylisoquinoline alkaloids from Alseodaphne corneri Kosterm, Asian Pac. J. Trop. Med. 9 (4) (2016) 328–332.
[62] A. Patra, A.J. Freyer, H. Guinaudeau, M. Shamma, B. Tantisewie, K. Pharadai, The bisbenzylisoquinoline alkaloids of Stephania suberosa, J. Nat. Prod. 49 (3) (1986) 424–427.